PHYSICAL REVIEW B VOLUME 8, NUMBER 1 1 JULY 1973

Low-Temperature Mössbauer Study of a Nickel-Zinc Ferrite: $Zn_xNi_{1-x}Fe_2O_4$

L. K. Leung
Department of Physics, University of Manitoba, Winnipeg 19, Manitoba, Canada

B. J. Evans
Department of Geology and Mineralogy, University of Michigan, Ann Arbor, Michigan 48104

A. H. Morrish
Department of Physics, University of Manitoba, Winnipeg 19, Manitoba, Canada

(Received 12 May 1972)

The Yafet-Kittel angles of the disordered system $Zn_xNi_{1-x}Fe_2O_4$ for $0 \leq x \leq 1$ have been determined using Fe^{57} Mössbauer spectroscopy with and without an external magnetic field. It is found that for $x \leq 0.5$ the resultant A- and B-site Fe-spin moments have a collinear arrangement, whereas for $x > 0.5$ a noncollinear arrangement of A- and B-site Fe spin moments exists. The canting angles of the B-site Fe moments determined from the applied-field Mössbauer spectra are smaller than those deduced from the neutron-diffraction data. An explanation based on the relative strength of the exchange constants J_{AB} and J_{BB} is given to account for this difference. The cation distributions are shown to correspond within experimental error limits to $(Zn_xFe_{1-x})[Ni_{1-x}Fe_{1+x}]O_4$ for all values of x in the interval $0 \leq x \leq 1.0$. The systematics of the dependence of the isomer shifts on Zn content are consistent with the variations in crystal chemical-structural parameters and with an increase in the covalence of the Fe^{2+}–O^{2-} bond with decreasing internuclear separation. The variations in the magnetic hyperfine fields at the A-site Fe ions can be understood on the basis of a molecular-field model with distant-neighbor exchange interactions being important at low temperatures. A significant contribution from supertransferred hyperfine interactions must be invoked to understand the systematics of the magnetic hyperfine field at the B-site Fe ions.

I. INTRODUCTION

In recent years there has been a considerable revival of interest in the properties of magnetically disordered ferrites.[1–9] In particular, there have been several neutron-diffraction and Mössbauer studies of the nickel-zinc ferrite, $Ni_{1-x}Zn_xFe_2O_4$, system.[10–13] As a consequence of these studies, it has been proven that, first of all, there is a canting among spins of the B-site ions, and second, that the concentration of paramagnetic Fe^{3+} ions, either as single ions or clusters, is nowhere near as great as previously expected.[14] In addition, a local-molecular-field model has been used to explain the saturation magnetization of the Ni-Zn ferrite system with considerable improvements over previous attempts.[15] This particular treatment of the saturation moments did not, however, allow for spin canting and there are small, but significant, deviations between the calculated and experimental moments at high-Zn contents.

Although considerable advancement in our understanding of the magnetic properties of the Ni-Zn ferrites has resulted from the above-mentioned studies, nevertheless there are still some cogent questions that remain to be answered. The correct interpretation of some of the recently generated results also needs to be clarified and confirmed by additional independent measurements. In addition, it is felt that it would be desirable to establish the corroborative aspects of the more recent results by performing several different kinds of measurements, e.g., magnetic, chemical, crystallographic, and Mössbauer, on identical specimens from chemically and structurally well-characterized parent materials.

Most important among some of the unanswered questions is the precise meaning of the canting angles deduced from the neutron-diffraction studies. It is obvious that the neutron-diffraction data permit one to deduce only the *average* canting angle among the B-site spins. No information is obtained regarding the local canting angles of the spins of the Ni^{2+} and Fe^{3+} B-site ions. In principle, the canting angles of the Ni^{2+} and Fe^{3+} ions are expected to be different on a local basis since the B-B and A-B exchange interactions J_{BB} and J_{AB} are known to be different for Ni^{2+} and Fe^{3+}.[9,16] In this regard, it is significant that the extrapolated canting angle of 90°, based on the neutron-diffraction data, for the B-site Fe^{3+} spins at $x=1$ is apparently not in agreement with the observed, rather complicated, spin structure of $ZnFe_2O_4$.[17] We have, therefore, determined the canting angle of the Fe^{3+} spins by means of Fe^{57} Mössbauer spectroscopy in external magnetic fields. We find that there are indeed differences between the (average) canting angles of the B-site Fe^{3+} spins, determined using Mössbauer spectroscopy, and the average canting angles of all the B-site spins, determined

using neutron diffraction. The relative magnitudes of the (average) Ni^{2+} and Fe^{3+} canting angles are qualitatively consistent with predictions based on the relative strengths of the exchange interactions within the local-molecular-field approximation.

Second, there is the question of the cation distribution. Through the improved resolution of the A- and B-site Fe^{57} Mössbauer spectra at low temperatures and in external magnetic fields, we have determined the cation distribution at 7 °K. The accuracy of the resulting cation distributions is not limited by differences in the recoilless fractions at the A and B sites, f_A and f_B, since f_A/f_B is expected to be very close to 1.00 at 7 °K[18]; and at the count levels employed in this study, inaccuracies in the absorption from which the cation distributions are deduced will not be greater than 1%.

The possibility of local fluctuations in the magnetic properties of the Fe^{3+} ions at low temperatures, i.e., 7 °K, is also considered on the basis of a local-molecular-field model and local variations in the supertransferred hyperfine interactions. Linewidth considerations indicate that variations in the hyperfine fields at Fe^{3+} ions due to local variations in molecular-field parameters are small. From the monotonic decrease at low temperature in the magnitude of the hyperfine fields at the B-site Fe^{3+} ions, however, it is concluded that there are substantial variations in the supertransferred hyperfine interactions at $Fe^{3+}(B)$ as the Zn content is varied.

Finally, to assure that the present data have some relevance to other studies, we have characterized each specimen in terms of its lattice parameter, chemical composition, saturation magnetization, and Néel temperature. The results of these characterizations indicate that the materials used in this investigation are similar to those used in previous studies; there are, however, quantitative differences between these and previous characterizations data.[10,12] We can therefore be confident that points of differences and similarities between the results of the present study and previous ones are substantive and not due to gross differences in the materials under investigation.

II. EXPERIMENTAL

The ferrite specimens were prepared by wet grinding into intimate mixtures carefully weighed powders of $ZnCO_3$, $NiCO_3$, and Fe_2O_3 (Johnson-Matthey Specpure grade) in relative amounts corresponding to the desired composition of the spinel ferrite. The mixtures of powders were pressed into pellets and fired at 1000 °C in a muffle furnace. The pellets were quenched in air, ground into a fine powder, repelletized, and refired at (1200–1300) °C; this sequence of operations was repeated until a single-phase material was obtained, as determined by x-ray powder diffractometry.

The chemical compositions of the samples were determined using wet-chemical techniques. Since the possibility of loss through volatilization is significant mainly for Zn, only the Zn content was determined in the wet-chemical analyses.[19] The closeness of the experimental weight percentages of the more volatile zinc to the nominal weight percentages makes it unlikely that the Ni and Fe contents are very different from their nominal values, and consequently the Ni and Fe contents were not determined.

The lattice constants were determined using Mn-filtered Fe$K\alpha$ radiation, a powder diffractometer,[20] and Si as an internal standard.

The saturation magnetization and Néel temperatures were determined using a vibrating-sample magnetometer in conjunction with a high-temperature vacuum furnace and low-temperature cryostat.[21]

The Mössbauer spectra were obtained using a constant-acceleration velocity transducer[22] and one-half of the memory of a 1024-channel multichannel analyzer[23] operated in the multiscaling or so-called "time mode." The spectrometer was calibrated using Fe-metal foil. For measurement of the spectra in an external field, a superconducting solenoid was used. The magnetic field axis was parallel to the direction of propagation of the γ rays. Both the source and velocity transducer were carefully shielded from the fringing field of the solenoid; the field at the source was less than 50 Oe. The Mössbauer source was Co^{57} in Cr. The absorbers were prepared by mixing the ferrite powders with a thermosetting plastic and hot pressing into $1\frac{1}{4}$-in.-diam disks. The thicknesses varied between 3 and 6 mg of Fe per cm^2. All spectra were obtained in transmission geometry and the 14.4-keV γ rays were monitored using an argon-methane-filled proportional counter. The source-detector distance was always large enough that geometrical broadening of the absorption lines was negligible.

III. RESULTS

The results of the chemical and x-ray analyses are presented in Table I, Fig. 1, and Table II, respectively. The zinc weight percentages of the various specimens are quite close to their nominal values, even though there does appear to be some slight loss of zinc, as expected. The lattice constants for the specimens used in this study are given in Table II; they are compared with other previously reported values in Fig. 1.

The saturation moments, magnetizations, and Néel temperatures are presented in Figs. 2–4, along with some previously reported determinations.[24–26] The agreement with previously pub-

TABLE I. Data on chemical analyses for Ni-Zn ferrite.

Nominal formulas	Zinc weight percent found	expected
$(Zn_{0.6}Fe_{0.4})[Ni_{0.4}Fe_{1.6}]O_4$	16.9 ± 0.2	16.5
$(Zn_{0.7}Fe_{0.3})[Ni_{0.3}Fe_{1.7}]O_4$	18.9 ± 0.1	19.2
$(Zn_{0.8}Fe_{0.2})[Ni_{0.2}Fe_{1.8}]O_4$	21.6 ± 0.2	21.8
$(Zn_{0.9}Fe_{0.1})[Ni_{0.1}Fe_{1.9}]O_4$	23.5 ± 0.1	24.4

TABLE II. Lattice constants of Ni-Zn ferrite.

Sample formula	a (Å)[a] (± 0.005)
$(Fe)[NiFe]O_4$	8.340
$(Zn_{0.1}Fe_{0.9})[Ni_{0.9}Fe_{1.1}]O_4$	8.351
$(Zn_{0.2}Fe_{0.8})[Ni_{0.8}Fe_{1.2}]O_4$	8.365
$(Zn_{0.3}Fe_{0.7})[Ni_{0.7}Fe_{1.3}]O_4$	8.378
$(Zn_{0.4}Fe_{0.6})[Ni_{0.6}Fe_{1.4}]O_4$	8.386
$(Zn_{0.5}Fe_{0.5})[Ni_{0.5}Fe_{1.5}]O_4$	8.399
$(Zn_{0.6}Fe_{0.4})[Ni_{0.4}Fe_{1.6}]O_4$	8.405
$(Zn_{0.7}Fe_{0.3})[Ni_{0.3}Fe_{1.7}]O_4$	8.417
$(Zn_{0.8}Fe_{0.2})[Ni_{0.2}Fe_{1.8}]O_4$	8.425
$(Zn_{0.9}Fe_{0.1})[Ni_{0.1}Fe_{1.9}]O_4$	8.432
$(Zn)[Fe_{2.0}]O_4$	8.442

[a]Determined from (533) diffraction peak with internal Si standard.

lished data is again seen to be rather good. Where there are slight differences between the values found in this study and those of previous ones, we believe them to be due to differences in the *actual* chemical compositions of the materials studied.

The Mössbauer spectra are shown in Figs. 5 and 6. The solid lines through the data points are the results of a least-squares fit to the data of two mixed magnetic-dipole and electric-quadrupole Fe^{57} hyperfine patterns. A least-squares-fitting program developed by Powell[27] and adapted to Mössbauer spectroscopy was used in the data analysis. The shapes of the lines were assumed to be Lorentzian and their intensities and widths were allowed to vary freely subject only to the constraints that $I_j = I_{7-j}$ and $\Gamma_j = \Gamma_{7-j}$, where I_j is the intensity of line j and Γ_j is the width of line j. For the zero-field spectra the relative integrated intensities of the lines of the two patterns were further constrained to have the values according to the cation distribution $(Zn_xFe_{1-x})[Ni_{1-x}Fe_{1+x}]O_4$. The linewidths, however, were allowed to be variable in every case subject only to the $\Gamma_j = \Gamma_{7-j}$ constraint. The above constraints do not apply for $x = 1.0$, where a six-line pattern is assumed and no constraints on the linewidths and on the intensities are used.

The parameters derived from the least-squares fits are listed in Tables III and IV. They are also plotted in Figs. 7–12. The area ratios and angles θ between the external field and B-site Fe^{3+} hyperfine-field directions were derived from the applied-field spectra obtained at 7 °K which are shown in Fig. 6. The angles have been derived from the data by two independent methods. In the first method, θ is deduced from the relative integrated

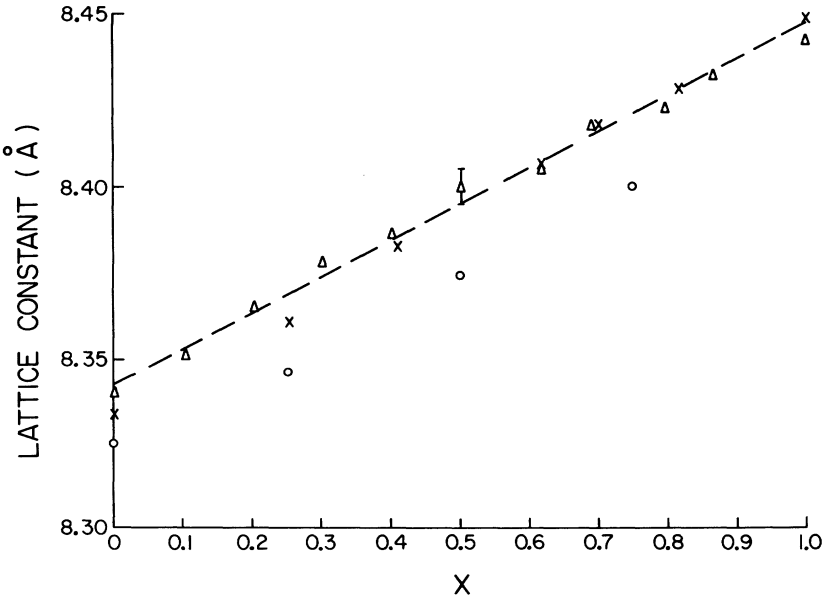

FIG. 1. Lattice constants vs x values. (×): data from Daniels and Rosencwaig (Ref. 13); (○): data from Satya Murthy *et al.* (Ref. 11); and (△): data from this work. The dashed line emphasizes the linearity of the data.

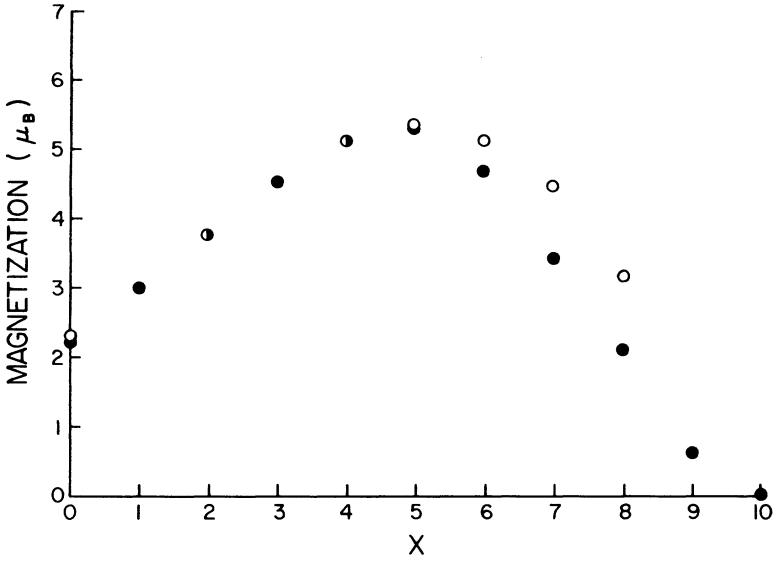

FIG. 2. Saturation magnetization at 4.2 °K vs x values. (O) represents data from Guillaud *et al.* (Ref. 24) for $H \to \infty$ and (●) represents data from this work for $H \to 0$.

intensities of the lines. The integrated intensities A_i of the lines are related to θ by the following equations:

$$A_{1,6} = 3(1+\cos^2\theta)\,, \quad A_{2,5} = 4\sin^2\theta\,, \quad A_{3,4} = (1+\cos^2\theta)\,, \tag{1}$$

where $A_{i,j}$ is the integrated intensity of lines A_i and A_j (since ideally $A_i = A_j$). We have evaluated the angle θ from the following relationship:

$$\theta = \arcsin\left(\frac{\frac{3}{2}(A_{2,5}/A_{1,6})}{1+\frac{3}{4}(A_{2,5}/A_{1,6})}\right)^{1/2}\,. \tag{2}$$

In the second method, we have used the relationship expressed in the following equation, which

TABLE III. Results of data analyses based on the zero-field spectra shown in Figs. 5(a) and 5(b).

	$H_{eff}(A)$ (kOe)	$H_{eff}(B)$ (kOe)	I.S. (A) (mm/sec)	I.S. (B)[a] (mm/sec)	$\frac{1}{4}e^2qQ(A)$ (mm/sec)	$\frac{1}{4}e^2qQ(B)$ (mm/sec)	$\Gamma(A)$ (mm/sec)	$\Gamma(B)$ (mm/sec)
0	511 ± 5	553 ± 5	0.60 ± 0.01	0.72 ± 0.01	−0.009 ± 0.004	−0.007 ± 0.004	0.50 ± 0.01	0.48 ± 0.01
0.2	510 ± 5	531 ± 5	0.59 ± 0.01	0.69 ± 0.01	−0.004 ± 0.006	−0.006 ± 0.006	0.44 ± 0.02	0.63 ± 0.03
0.3	511 ± 5	530 ± 5	0.54 ± 0.01	0.64 ± 0.01	−0.027 ± 0.007	0.008 ± 0.005	0.48 ± 0.04	0.61 ± 0.02
0.4	509 ± 5	523 ± 5	0.55 ± 0.03	0.58 ± 0.03	−0.07 ± 0.02	0.02 ± 0.01	0.43 ± 0.04	0.55 ± 0.03
0.5	504 ± 5	521 ± 5	0.57 ± 0.05	0.62 ± 0.05	−0.07 ± 0.03	−0.01 ± 0.01	0.55 ± 0.10	0.58 ± 0.05
0.6	505 ± 5	517 ± 5	0.55 ± 0.05	0.52 ± 0.05	−0.14 ± 0.02	0.01 ± 0.01	0.49 ± 0.03	0.52 ± 0.04
0.7	505 ± 5	512 ± 5	0.54 ± 0.05	0.54 ± 0.05	−0.24 ± 0.01	0.002 ± 0.004	0.35 ± 0.06	0.56 ± 0.02
0.8	507 ± 5	514 ± 5	0.54 ± 0.05	0.59 ± 0.05	−0.17 ± 0.04	0.016 ± 0.003	0.27 ± 0.02	0.59 ± 0.01
0.9	506 ± 5	487 ± 5	0.62 ± 0.05	0.60 ± 0.05	−0.001 ± 0.01	−0.039 ± 0.006	0.28 ± 0.03	0.83 ± 0.06
1.0	•••	454 ± 5	•••	0.67 ± 0.02	•••	0.03 ± 0.02	•••	1.30 ± 0.07
1.0[b]	•••	486 ± 5	•••	0.65 ± 0.01	•••	0.005 ± 0.003	•••	0.81 ± 0.01

[a]With respect to Cr.

[b]Done at 4.2 °K.

was also used by Chappert and Frankel[1] in a Mössbauer study of spin canting in $NiFe_2O_4$ and $NiFe_{2-x}Cr_xO_4$:

$$\theta = \arccos\{[H_n^2(B) - H_{ext}^2 - H_{hf}^2(B)]/[2H_{ext}H_{hf}(B)]\} . \quad (3)$$

$H_{hf}(B)$ is the hyperfine field at the B-site Fe^{3+} ions in zero external field; $H_n(B)$ is the hyperfine field at the B-site Fe^{3+} ion in the presence of an external field, and H_{ext} is the external field. As seen in Table V, for $x \leq 0.8$ there is good agreement between the angles deduced from Eqs. (2) and (3); there is a divergence, though, between the angles deduced using the two methods for $x > 0.8$.

IV. DISCUSSION

The chemical compositions, lattice constants, and magnetic-properties data serve mainly to establish the relevance of the present study to previous ones. In the main, the Ni-Zn ferrites of this study are comparable with the ferrites used in previous ones. The complete delineation of the physical properties serve the further purpose of permitting other investigators to easily test the important conclusions of this study.

Most of the previous Mössbauer studies of Ni-Zn ferrites have been concerned with relaxation phenomena, and cogent aspects of the 0 °K behavior have been neglected. Therefore, our main concern in this study has been the cation distributions, magnetic structures, and their implications for local-molecular-field models and exchange interactions in disordered spinel ferrites at 0 °K. We have also devoted some attention to systematic differences between the results of this and previous studies. The remainder of our discussion will be devoted to these topics.

A. Cation Distributions

First of all, as seen in Fig. 8 and Table IV, excellent agreement is obtained between the experimental integrated intensity ratios of the A- and B-site Fe^{57} spectra and those calculated on the basis of the cation distribution $(Fe_{1-x}Zn_x)[Ni_{1-x}Fe_{1+x}]O_4$. The slight deviation at high-x values is believed to be due to poor resolution of the spectra (cf. Fig. 6) even in the external magnetic field. Since these measurements were made on thin absorbers at 7 °K, corrections for finite thicknesses and differences in recoilless fractions are negligible. Previous Mössbauer studies on the spinel ferrites $NiFe_2O_4$,[28] Fe_3O_4,[18] γ-Fe_2O_3,[29] $CuFe_2O_4$,[30] and $LiFe_5O_8$[31a] have all shown $f_A/f_B \cong 1.0$ at 4.2 °K. In this study the cation distribution has been shown to be $(Fe_{1-x}Zn_x)[Fe_{1+x}Ni_{1-x}]O_4$ in nickel-zinc ferrites for all values of x between 0 and 1. Perhaps there was little doubt before this study concerning the qualitative aspects of the cation dis-

TABLE IV. Results of data analyses based on the applied-field spectra shown in Figs. 6(a) and 6(b).

x	$H_{eff}(A)$ (kOe)	$H_{eff}(B)$ (kOe)	I.S.$(A)^a$ (mm/sec)	I.S.$(B)^a$ (mm/sec)	$\frac{1}{4}e^2qQ(A)$ (mm/sec)	$\frac{1}{4}e^2qQ(B)$ (mm/sec)	$\Gamma_{1,6}(A)$ (mm/sec)	$\Gamma_{1,6}(B)$ (mm/sec)	$\Gamma_{2,5}$ (mm/sec)	Area (A) / Area $(B)_{th}$	Area (A) / Area $(B)_{expt}$
0.2	558 ± 5	485 ± 5	0.56 ± 0.01	0.65 ± 0.01	−0.004 ± 0.006	0.01 ± 0.01	0.42 ± 0.02	0.61 ± 0.03	0	0.67	0.61 ± 0.10
0.3	559 ± 5	481 ± 5	0.57 ± 0.01	0.68 ± 0.01	−0.01 ± 0.01	0.01 ± 0.01	0.44 ± 0.02	0.59 ± 0.01	0	0.54	0.51 ± 0.03
0.4	559 ± 5	472 ± 5	0.56 ± 0.01	0.69 ± 0.01	0.01 ± 0.01	0.008 ± 0.004	0.41 ± 0.02	0.61 ± 0.01	0	0.43	0.39 ± 0.03
0.5	555 ± 5	466 ± 5	0.57 ± 0.01	0.68 ± 0.01	0.01 ± 0.01	−0.002 ± 0.005	0.42 ± 0.04	0.60 ± 0.01	0	0.33	0.33 ± 0.03
0.6	559 ± 5	466 ± 5	0.55 ± 0.01	0.67 ± 0.01	0.00 ± 0.02	−0.006 ± 0.004	0.45 ± 0.05	0.63 ± 0.03	0.32 ± 0.13	0.25	0.24 ± 0.05
0.7	560 ± 5	470 ± 5	0.54 ± 0.01	0.67 ± 0.01	0.01 ± 0.04	0.008 ± 0.004	0.55 ± 0.05	0.71 ± 0.02	1.01 ± 0.12	0.18	0.22 ± 0.05
0.8	564 ± 5	472 ± 5	0.54 ± 0.01	0.62 ± 0.01	−0.03 ± 0.03	0.002 ± 0.007	0.76 ± 0.08	0.84 ± 0.03	0.80 ± 0.05	0.11	0.23 ± 0.07
0.9	547 ± 5	465 ± 5	0.60 ± 0.01	0.66 ± 0.01	0.04 ± 0.03	−0.005 ± 0.009	0.63 ± 0.11	0.84 ± 0.03	1.15 ± 0.06	0.05	0.12 ± 0.09
1.0	...	446 ± 5	...	0.67 ± 0.01	...	0.02 ± 0.02	...	1.33 ± 0.11	1.16 ± 0.11	0	0

[a]With respect to Cr.

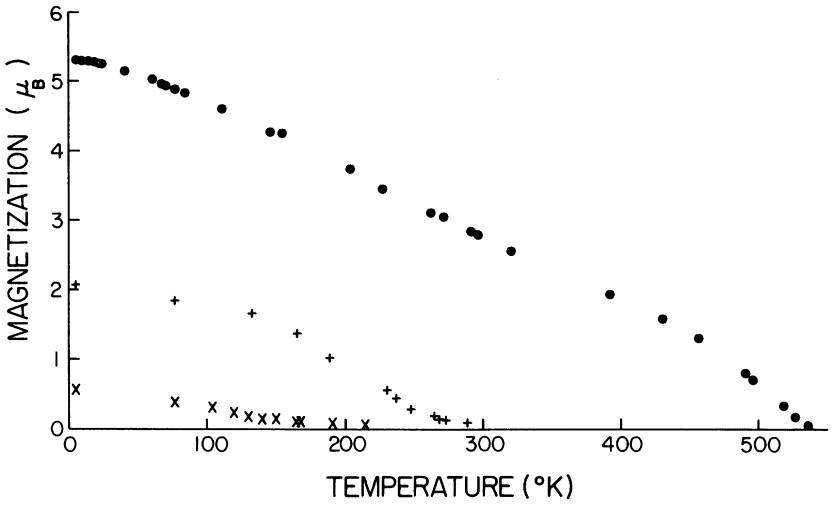

FIG. 3. Saturation magnetization as a function of temperature for three compositions: (●) for $x=0.5$; (+) $x=0.8$; and (×) $x=0.9$.

tribution in $Ni_{1-x}Zn_xFe_2O_4$. It is reassuring that good quantitative agreement is obtained, especially since it has been suggested that a small amount of Zn^{2+} occupies the B sites in rapidly cooled $ZnFe_2O_4$[31b] and in the ternary system $NiFe_2O_4$-$ZnFe_2O_4$-Ni_2GeO_4.[31c] This result permits a consideration of the local magnetic properties in terms of the statistics of the cation distribution to be undertaken with confidence.

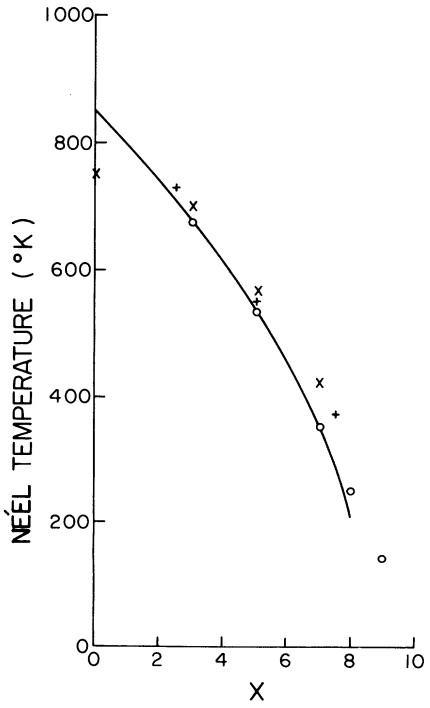

FIG. 4. Néel temperature vs x values. The solid curve represents data from Piskarev (Ref. 25), (×) from Booth and Crangle (Ref. 26), (+) from Satya Murthy *et al.* (Ref. 11), and (○) from this work.

B. Magnetic Hyperfine Fields

None of the previous Mössbauer measurements on the Ni-Zn ferrites have succeeded in fully resolving the A- and B-site patterns at several values of x, as has been done in the present study. Most of the data in this study on the hyperfine fields H_{hf} are therefore *not directly* comparable with those of earlier ones. The two most extensive Mössbauer studies on Ni-Zn ferrites have been those of Goldanskii *et al.*[12] and Daniels and Rosencwaig.[13] In these two papers, there was disagreement in the dependence of H_{hf} on x. Goldanskii *et al.* used no external field at all, and the strength of the field (13.6 kOe) employed by Daniels and Rosencwaig was insufficient to fully resolve the A and B patterns. Hence there existed uncertainty in these deductions concerning the hyperfine field. We do observe without ambiguity that the B-site hyperfine field does indeed decrease faster as a function of x than the A-site hyperfine field *at* 7 °K, a result qualitatively similar to that given in Ref. 13 based on spectra obtained at 77 °K. From our applied field spectra at 7 °K which are the most reliable for studying the varia-

TABLE V. Average Yafet-Kittel angles for $(Zn_xFe_{1-x})[Ni_{1-x}Fe_{1+x}]O_4$.

x	$\bar{\theta}_{YK}(B)$ [Eq. (2)]	$\bar{\theta}_{YK}(B)$ [Eq. (3)]
0→0.5	0	0
0.6	18°± 5°	20°± 5°
0.7	32°± 5°	32°
0.8	39°± 5°	41°
0.9	52°± 10°	61°
1.0	59°± 15°	79°

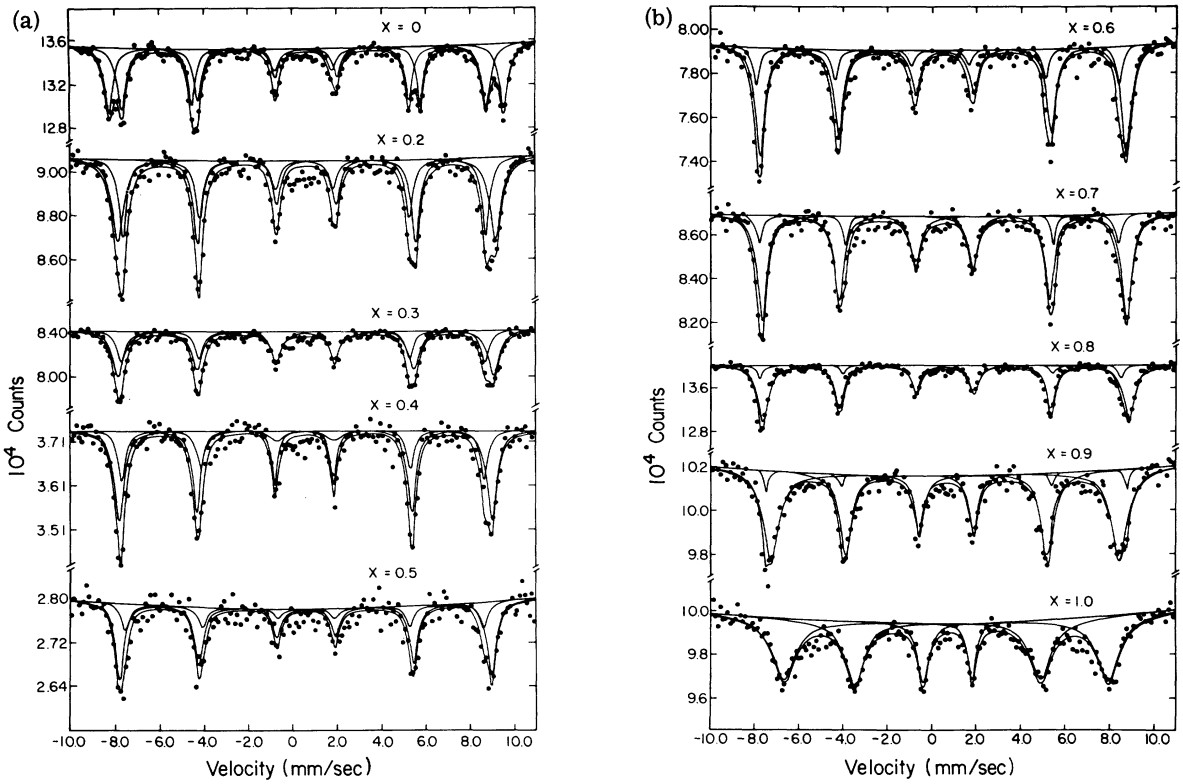

FIG. 5. Mössbauer spectra of $Zn_xNi_{1-x}Fe_2O_4$ at 7 °K. The solid curves are the least-squares computer fits.

tion in hyperfine fields, it is concluded (cf. Fig. 10) that the B-site field is larger than the A-site field up to $x \cong 0.7$ and is only slightly smaller than the A-site field for $x > 0.7$, the difference being within the experimental error and of little significance. The crossover point found in Ref. 13 at 77 °K was at $x = 0.4$ and the B-site field was smaller than the A-site field by slightly more than 20 kOe at $x = 0.6$. The difference in the x values at which $H_{hf}(A) > H_{hf}(B)$ as obtained in the present study and in Ref. 13 are probably due largely to the difference in the temperatures at which the measurements were made.

The results of the present study at 7 °K show the same relative dependence of $H_{hf}(A)$ and $H_{hf}(B)$ on x as was obtained in a more precise NMR study of $Ni_{1-x}Zn_xFe_2O_4$ at 77 °K[32]; namely, $H_{hf}(A)$ is essentially independent of x for $x \leq 0.4$ at 77 °K[32] and is also independent of x for $x \leq 0.9$ at 7 °K as determined in the present study. On the other hand, $H_{hf}(B)$ is strongly dependent on the value of x.

We believe the supertransferred hyperfine interactions provide a tractable explanation of these effects. The same conclusion was also reached in the study of the Co-Zn ferrites.[33] These effects will be discussed below.

It is also clear that the smaller magnitude of $H_{hf}(A)$ compared to $H_{hf}(B)$ in pure $NiFe_2O_4$ is due primarily to covalency, as previously suggested for inverse spinel ferrites.[3,29,30] The reduced magnetization $\sigma(298\ °K)/\sigma(0\ °K)$ of the A sublattice is larger than that of the B sublattice to at least 298 °K, $\sigma(298\ °K)/\sigma(0\ °K)$ being 0.970 for the A site and 0.960 for the B site[32,34,35]; and the fact that $H_{hf}(B) > H_{hf}(A)$ cannot be attributed to any great degree to local-molecular-field effects. It is true, of course, that the absolute values of the magnetic moment and/or H_{hf} are larger for the B Fe ions than for A Fe ions, but this is due mainly to the greater covalence and consequently greater degree of spin delocalization at the A site. Furthermore, as shown in Figs. 10 and 12, we observe a very weak dependence of $H_{hf}(A)$ on x for $0 \leq x \leq 0.8$ at 7 °K, $H_{hf}(A)$ being constant within the experimental error of ± 5 kOe. Our data are in good agreement with the NMR measurement at 77 °K for $0 \leq x \leq 0.4$; the difference in the range of x values over which $H_{hf}(A)$ is constant being due primarily to the difference in temperatures. In addition to these results, the x dependence of the linewidths (Fig. 9) and relative magnitudes of $H_{hf}(A)$ and $H_{hf}(B)$ all indicate that the influence of the B-site-cation disorder in $Ni_{1-x}Zn_xFe_2O_4$ does not make for appreciable changes in $H_{hf}(A)$. Measurements on pure and

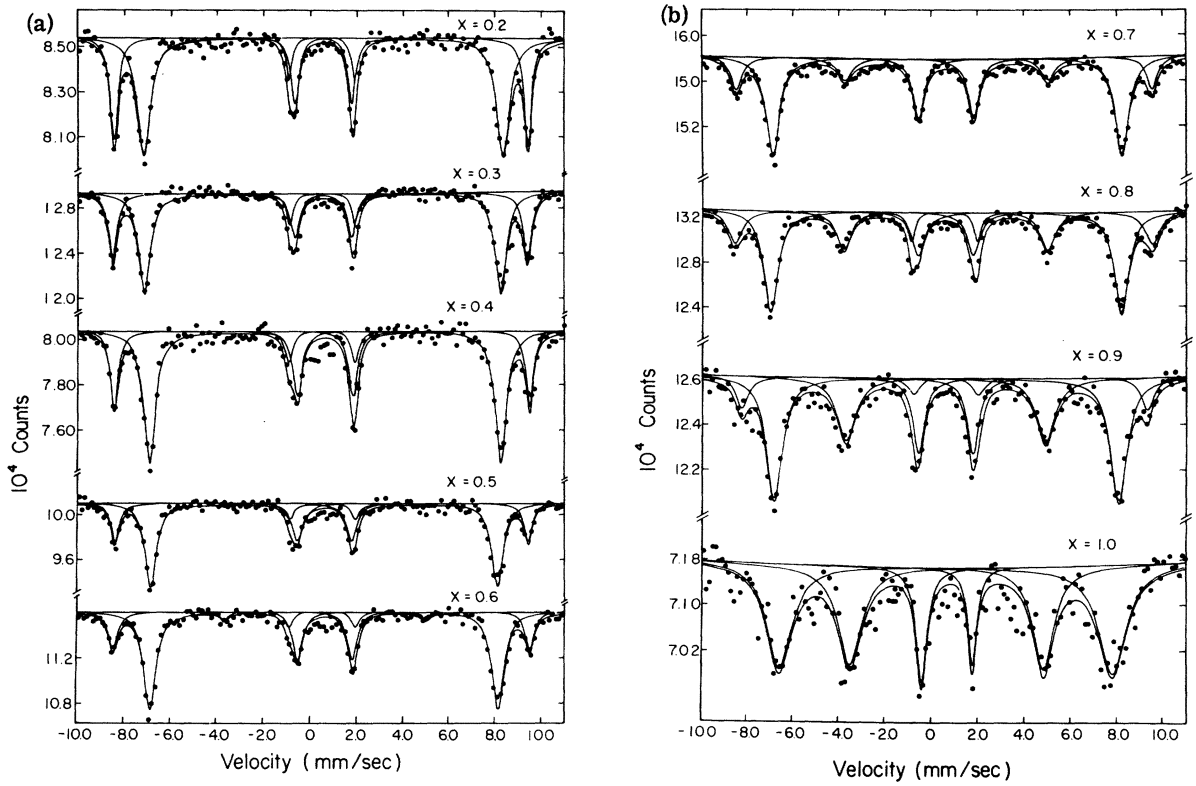

FIG. 6. Mössbauer spectra of $Zn_xNi_{1-x}Fe_2O_4$ at 7 °K with an external field of 50 kOe parallel to the direction of propagation of the γ ray. The solid curves are the computer fits.

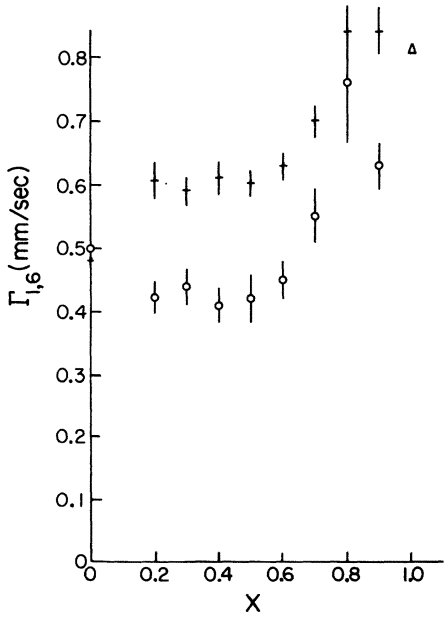

FIG. 7. Outermost linewidth ($\Gamma_{1,6}$) vs x values. (○) represents data corresponding to the A site at 7 °K; (+), B-site at 7 °K; and (Δ), B site at 4.2 °K. Data for $x=1.0$ at $T=7$ °K have been omitted because the ratio T/T_N is too large to be compatible with the data for $x<1.0$ at 7 °K.

Sb-substituted $LiFe_5O_8$ have shown quantitatively that even for diamagnetic B-site ions the influence of cation disorder on $H_{hf}(A)$ is quite small.[31a]

We have chosen not to attempt a quantitative fit of a local-molecular-field model to the Mössbauer spectra (as was done, for example, in Ref. 33) for a number of compelling reasons. First of all, there is no observable structure in the B-site spectra which can be used to judge the adequacy of such fittings. Second, complications are expected to arise from the fact that both Ni^{2+} and Zn^{2+} can influence the hyperfine fields in rather different manners. Some of these complications have already been encountered in the Co-Zn ferrites in which the behavior of Co^{2+} is apparently anomalous.[33] Third, unlike the case in which one has to consider only Fe^{3+} and one other diamagnetic cation, the supertransferred hyperfine effects and purely molecular-field effects may have both qualitative and quantitative differences when two kinds of magnetic ions are present. In this case the distribution in the magnitudes of hyperfine fields and the frequency of their occurrence can be quite complicated. Again, some of these complications appear to have been present in the results on the Co-Zn ferrites.[33]

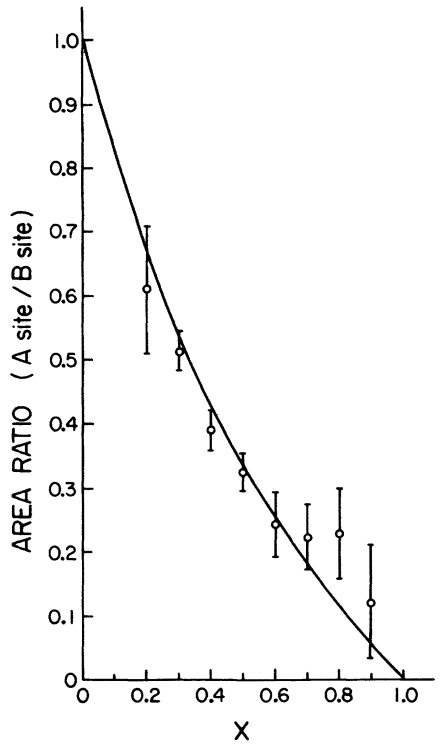

FIG. 8. Area ratio between A and B site vs x values. (○) represents experimental data and the solid curve is calculated based on the cation distribution $(Zn_xFe_{1-x})[Ni_{1-x}Fe_{1+x}]O_4$.

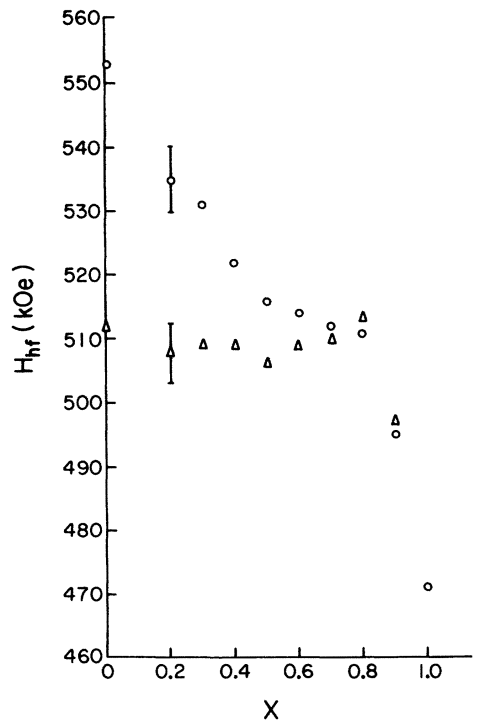

FIG. 10. Hyperfine fields derived from Figs. 6(a) and 6(b) after correcting for the external field. (○) represents data corresponding to B site and (△) the A site.

C. Isomer Shifts

As seen in Fig. 9 and Table IV both the absolute and relative values, i.e., [I.S.(B) − I.S.(A)], of the isomer shifts are insensitive to the Zn content: The differential isomer shift [I.S.(A) − I.S.(B)] is essentially constant within experimental error for $0 \leq x \leq 0.7$, where the spectra are still well resolved in the external field. A similar observation was made in Ref. 13 on less well-resolved spectra. The value of 0.12 ± 0.02 mm/sec for [I.S.(A) − I.S.(B)] over the entire composition range is in good agreement with previous estimates of the differential octahedral-tetrahedral isomer shifts in spinel ferrites.[3,28,30,31a] The insensitivity of [I.S.(B) − I.S.(A)] to x is not surprising. Any variations in the magnitudes of this quantity at 7 °K are expected to be due to differences in the Fe^{3+}-O^{2-} internuclear separations, and the variations in the Fe^{3+}-O^{2-} internuclear separations are small. Using the recently reported u parameter of 0.3855 ± 0.0005 and 0.3823 ± 0.0003 for $ZnFe_2O_4$[36] and $NiFe_2O_4$,[37a] respectively, the Fe^{3+}-O^{2-} internuclear separations are as follows: for $ZnFe_2O_4$, r_{AO} is 1.966 Å and r_{BO} is 2.018 Å; and for $NiFe_2O_4$, r_{AO} is 1.911 Å and r_{BO} is 2.024 Å. Therefore, the B-site isomer shifts should be independent of x for all x values since $[r_{BO}(ZnFe_2O_4) - r_{BO}(NiFe_2O_4)]$ has a maximal value of 0.006 Å or is essentially constant for all x values. On the other hand, $[r_{AO}(ZnFe_2O_4) - r_{AO}(NiFe_2O_4)]$ is 0.055 Å and the A-site isomer shift should not be independent of

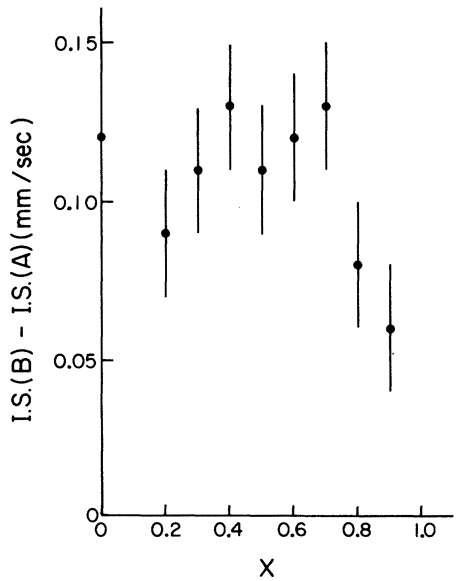

FIG. 9. Differential isomer shift vs x values.

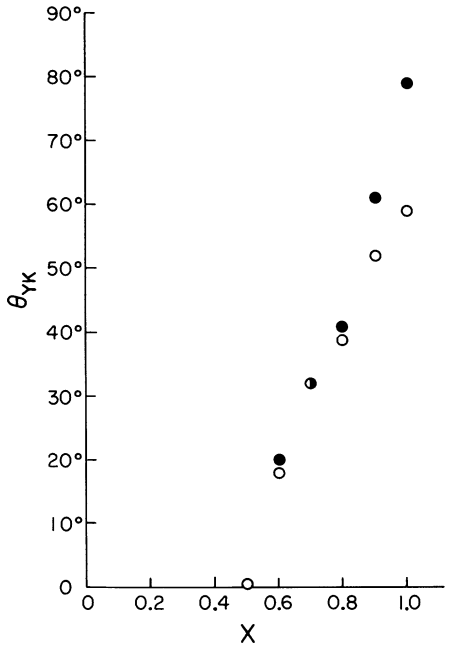

FIG. 11. Yafet-Kittel angle vs x values. (○) represents results obtained through Eq. (2) and (●), through Eq. (3); also compare Table V.

x for all x; this requires, of course, that [I.S. (A) − I.S. (B)] also not be independent of x for all values of x. Quantitatively, neutron-diffraction studies have shown that the u parameters of $Ni_{1-x}Zn_xFe_2O_4$ are insensitive to x for $x \leq 0.7$, at which the x value u begins to approach that appropriate to pure $ZnFe_2O_4$.[11] The constancy of [I.S. (A) − I.S. (B)] up to $x = 0.7$ is therefore easily explained on the basis of the constant values of r_{AO} and r_{BO}; the changes in [I.S. (A) − I.S. (B)] for $x > 0.7$ are therefore due to the changes in r_{AO}. That [I.S. (A) − I.S. (B)] decreases for $x > 0.7$ is explained on the basis of the internuclear separation as follows: The Fe^{3+}-O^{2-} r_{AO} value is greater for $x > 0.7$ than for $x \leq 0.7$; the covalence of the Fe^{3+}-O^{2-} A-site bond is therefore somewhat less for $x > 0.7$; this would, in turn, imply a greater value of I.S. (A) for $x > 0.7$ relative to I.S. (B) (since r_{BO} does not change even for $x > 0.7$). Hence, a decrease in [I.S. (A) − I.S. (B)] for $x > 0.7$ is predicted on this basis; and the prediction is borne out.

D. Linewidths

The linewidths of the Fe^{57} Mössbauer spectra are useful for estimating the influence of cation disorder on both the electric and magnetic interactions. Previous Mössbauer studies[12,13,37b] of the Ni-Zn ferrites have been made at temperatures too high for a reliable estimate to be made of the separate contributions of the cation disorder to the (i) electric and (ii) magnetic interactions; the influence of the magnetic interactions has dominated the linewidth variations. In the present study, the measurement temperatures have been sufficiently low to minimize the magnetic effects. Except for the supertransferred hyperfine interactions, the linewidth variations are due exclusively to electric effects—e.g., electric-monopole and -quadrupole interactions. At all values of $x > 0$, the outermost lines of the B-site pattern, $\Gamma_{1,6}$, are broader than those of the A-site pattern. At $x = 0$, however, $\Gamma_{1,6}(B) \approx \Gamma_{1,6}(A)$. It has been shown[3] that the widths of the outermost lines (1 and 6) are about six times more sensitive than those of the innermost lines (3 and 4) to fluctuation effects in the magnitudes of the hyperfine field, whereas the widths of all of the lines are equally sensitive to variations in the quadrupole-coupling constant. The broadening of the B-site lines at 7 °K in $NiFe_2O_4$ due to the different values of $e^2qQ(3\cos^2\theta - 1)$, where θ is the angle between the principal axis of the electric-field-gradient tensor and the magnetic hyperfine field, is apparently of the same magnitude as any possible broadening of the A-site lines resulting from local variations in the $Fe^{3+}(A)$-O^{2-} − Me(B) exchange interactions (Me = Fe^{3+} or Ni^{2+}). The results of the present study are supported by recent Mössbauer measurements on $LiFe_5O_8$[31a] in which the outermost A-site linewidth is smaller than the

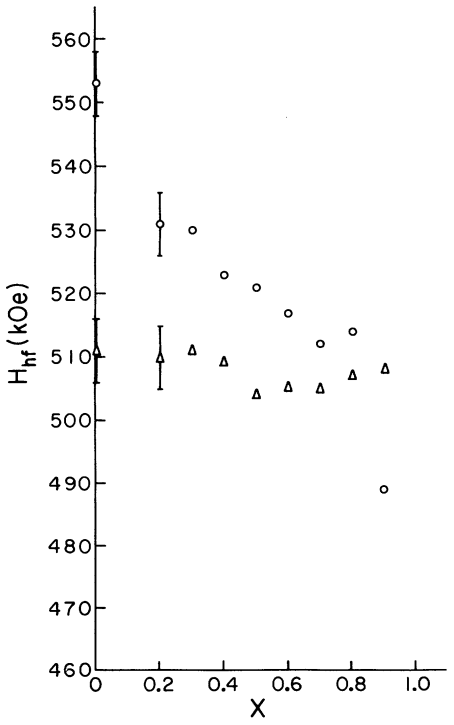

FIG. 12. Hyperfine fields derived from Figs. 5(a) and 5(b). (○) represents data corresponding to B site at 7 °K and (△), data at A-site at 7 °K.

B-site linewidth even though there is substantial disorder on the B site, and no disorder on the A sites to contribute to magnetic broadening of the linewidths of the B-site pattern. Further evidence against local fluctuations in $H_{hf}(A)$ as causing significant line broadening for $x < 0.6$ is provided by the constancy of Γ_A and Γ_B for $0.2 \leq x \leq 0.6$ (cf. Fig. 7). Γ_A would have been expected to decrease and Γ_B to increase with increasing x if local-molecular-field effects were important.

The constancy of Γ_B for $0.2 \leq x \leq 0.6$ is, however, *consistent* with quadrupole effects. The interpretation of the dependence of Γ_A and Γ_B on x for $0 \leq x \leq 0.6$ on the basis of the electric-quadrupole interaction goes as follows: For $x = 0$, the *spread* in magnitudes of the quadrupole interactions is greatest for the A-site ions and minimal for the B-site ions insofar as the magnitudes are determined by chemical order on the opposite sublattice. Upon the addition of Zn, this situation is reversed and the field gradients at the A-site ions would become more uniform as the B sites are occupied to a greater extent by Fe ions; consequently, Γ_A decreases. Conversely, the field gradient at B-site Fe^{3+} ions would become nonuniform and Γ_B would increase with increasing x. These considerations are valid for small x. Because the range of quadrupole splittings at Fe^{3+} ions in spinel ferrites is rather small, of the order of 0.5 mm/sec,[38,39] the broadening due to the nonuniform quadrupole interactions is expected to saturate rather rapidly as a function of x relative to the precision with which the linewidths can be determined. Hence, the constancy of Γ_A and Γ_B for $0.2 \leq x \leq 0.6$. For $x \geq 0.7$, the broadening of the lines is also believed to be partly due to isomer-shift fluctuations as explained in Sec. IV C. However, for $x \geq 0.8$, T/T_N at 7 °K is no longer small enough to ignore the local-molecular-field fluctuations and much of the line broadening in this region may be due to fluctuations in the magnetization at different Fe sites. This broadening mechanism is a macroscopic effect and would be important for both the A and B sites, as observed.

E. Spin Structure

One interesting result of the present study is the rather large deviations between the *average* canting angles of the B-site spin moments, determined using neutron diffraction,[11] and the *average* canting angle of the *B-site* Fe^{3+} *spin moments*, determined in the present study using Mössbauer resonance. While the doubtful could raise questions concerning the significance of these differences for angles determined on the basis of the relative intensities of lines 1 and 2 (5 and 6) of the Mössbauer spectra because of possible saturation effects, the fact that similar differences in the angles are obtained on the basis of the magnitudes of $H_n(B)$ and $H_{hf}(B)$ [cf. Eqs. (2) and (3) and Table V] definitely establishes these differences as being real. There is, in fact, an obvious difference (as implied above) in the meaning of the canting angles determined by the two techniques, aside from any commitment to the details of the three sublattice models used in the neutron-diffraction study[11] or to the details of our analysis of the Mössbauer data.

From the neutron-diffraction measurement one determines the average B-site canting angle $\bar{\theta}_{YK}$ which includes some weighted sum of the *average* canting angles of the Ni^{2+} spins, $\bar{\theta}_{YK}(Ni)_B$, and of the Fe^{3+} spins, $\bar{\theta}_{YK}(Fe)_B$, i.e.,

$$\bar{\theta}_{YK}^{ND}(B) = \bar{\theta}_{YK}(B) , \tag{4}$$

where

$$\bar{\theta}_{YK}(B) = C_1 \bar{\theta}_{YK}(Fe)_B + (1 - C_1)\bar{\theta}_{YK}(Ni)_B , \tag{5}$$

where $\bar{\theta}_{YK}^{ND}(B)$ is the canting angle determined using neutron diffraction. The canting angle $\bar{\theta}_{YK}$ determined from the Mössbauer data corresponds to the average canting angle of Fe spins only, i.e.,

$$\bar{\theta}_{YK}^{ME}(B) = \bar{\theta}_{YK}(Fe)_B , \tag{6}$$

where $\bar{\theta}_{YK}^{ME}(B)$ is the canting angle determined using Fe^{57} Mössbauer spectroscopy.

The smaller value of $\bar{\theta}_{YK}(Fe)_B$ compared to $\bar{\theta}_{YK}(B)$ can be qualitatively understood on the following basis: Since the strength and sign of the B-B exchange interactions relative to the A-B exchange interactions determine the canting angle[40] and since it is also known that the $Fe^{3+}(B)$-$Fe^{3+}(A)$ exchange interactions are about three times larger than the $Ni^{2+}(B)$-$Fe^{3+}(A)$ interactions,[41] it follows that $\bar{\theta}_{YK}(Ni)_B$ will in general be greater than $\bar{\theta}_{YK}(Fe)_B$. The possibility that the hyperfine-field directions are not collinear with the local spin moments need not be given serious consideration for the Fe^{3+} ion, which has little or no orbital contribution to its magnetic moment in the nickel-zinc ferrites.

While the above explanation accounts qualitatively for the relative magnitudes of $\bar{\theta}_{YK}(B)$ and $\bar{\theta}_{YK}(Fe)_B$,[8] there are still some further points to be considered regarding the magnitudes and precise interpretations of these angles. First, if it is true that $\bar{\theta}_{YK}(Ni)_B$ is different from $\bar{\theta}_{YK}(Fe)_B$ then the three-sublattice model of Satya Murthy *et al.*[12] is correct *only if the* Ni *and* Fe *atoms are randomly distributed over the two B-site magnetic sublattices*. In the case of random Ni and Fe occupations of the magnetic sublattices, the moments of the two B magnetic sublattices, B_1 and B_2, would be equal and the resultant B moment collinear with the A-site moment. The angle $\bar{\theta}_{YK}(Fe)_B$ between the Fe^{57} hyperfine field and external field directions

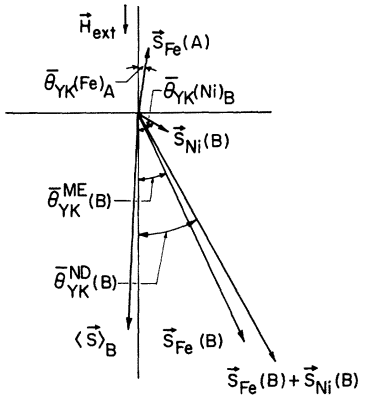

FIG. 13. Schematic diagram of the local-spin configuration in $Zn_xNi_{1-x}Fe_2O_4$ for $x>0.5$. Here $\langle\vec{S}\rangle_B=\frac{1}{2}(\vec{B}_1+\vec{B}_2)$, where $\vec{B}_i=\vec{S}_{Fe}(B_i)+\vec{S}_{Ni}(B_i)$ and $i=1,2$.

would still be less than $\bar{\theta}_{YK}(B)$, but $\bar{\theta}_{YK}(Fe)_A$ would be zero. On the other hand, if the Fe^{3+} and Ni^{2+} ions are not randomly distributed on B_1 and B_2, then the moments of B_1 and B_2 would not be equal and their resultant would not in general be parallel to the A-site moment. In this case, as in the previous case, the angle between the external-field and the hyperfine-field directions, $\bar{\theta}_{YK}(Fe)_B$, would not be equal to $\bar{\theta}_{YK}(B)$; however, $\bar{\theta}_{YK}(Fe)_A$ would not be zero. This spin arrangement and the resulting angles are depicted schematically in Fig. 13. The resultant magnetization, which lies along the external-field direction, is neither parallel to the A- or B-site spin moments, and two angles $\bar{\theta}_{YK}(Fe)_B$ and $\bar{\theta}_{YK}(Fe)_A$ must be determined from the Mössbauer data.

That the spin arrangement in Fig. 13 is probably the correct one for $(Fe_{1-x}Zn_x)[Ni_{1-x}Fe_{1+x}]O_4$ is indicated by the large values of $\Gamma_{2,5}$ relative to $\Gamma_{1,6}$ (cf. Table IV) and the fact that $\Gamma_{2,5}$ increases as a strong function of x even though $\Gamma_{1,6}$ is only weakly sensitive to changes in x. That this supports a noncollinear spin structure for the resultant of A and B spin moments follows from the requirement that $\Gamma_{2,5}$ should not be greater than nor as large as $\Gamma_{1,6}$ if the resultant B- and A-site moments are parallel to the external field[42]; yet from Table IV we see that $\Gamma_{2,5}$ is generally larger than $\Gamma_{1,6}$ for $x>0.5$. Lines 2 and 5 are also asymmetric indicating again contributions from two or more different lines. For the spin arrangement in $Ni_{1-x}Zn_xFe_2O_4$, at least for $0.5<x\leq 0.8$, we prefer that depicted in Fig. 13.

A similar spin arrangement was also deduced from the applied-field Mössbauer studies of $NiCr_{1.7}Fe_{0.3}O_4$[1] and also in a similar study of Zn-Co ferrites.[33] In these cases, however, external fields of sufficient magnitudes, e.g., $\simeq$80 kOe, to resolve the structure in lines 2 and 5 were available. We have not attempted any computer-assisted resolution of lines 2 and 5 into their A and B components since the intensities and fine structure in the peaks are too weak for reliable least-squares fitting. Our neglect of possible A-site canting has no effect on the qualitative conclusions of this study; $\bar{\theta}_{YK}(Fe)_B$ is still less than $\bar{\theta}_{YK}(B)$. The values for $\bar{\theta}_{YK}(Fe)_B$ determined in this study are, however, only upper limits to the canting angles of the Fe(B) spin moments.

F. Supertransferred Hyperfine Interactions

The variations in $H_{hf}(A)$ and $H_{hf}(B)$ as a function of Zn content, depicted in Figs. 10 and 12, confirm the conclusions of previous studies that $H_{hf}(A)$ is insensitive to the kinds and number of cations on the B sites.[3,31a,33] For these data, obtained at 7 °K, variations in H_{hf} due to a T/T_N effect are negligible, except perhaps for $x>0.8$. The variations in H_{hf} are therefore due largely to nondynamical effects and arise from changes in the supertransferred hyperfine interactions as the cation neighbors about a given Fe ion are changed.

The suggestion that local variations in H_{hf} due to supertransferred hyperfine interactions make significant contributions to the linewidths in spinel ferrites as observed in the Fe^{57} Mössbauer spectra has received careful consideration in Ref. 3 and more recently in Ref. 41. As noted in Ref. 3, the Fe^{57} data are difficult to interpret on a quantitative basis because of the presence of multiple-spin-transfer mechanisms, namely, overlap and covalence, and multiple-coupling paths, i.e., B-B vs A-B. This is still true despite recent semiempirical studies.[43,44] Qualitatively, however, spin transfer from an A-site Fe^{3+} ion via O^{2-} p orbitals into the 4s orbital of a B-site Fe^{3+} ion will increase the magnitude of H_{hf} above that observed in the absence of such supertransferred hyperfine interactions. Direct metal-metal overlap, again involving only the 4s orbital, would also lead to the same conclusion. In general, the effective magnetic hyperfine field H_{hf} is given by the expression below:

$$H_{hf}=H_c+H^{dil}_{cov}+H_{orb}+H_{zsd}+H_{dip}+H^{conc}_{cov}\ . \qquad (7)$$

H_c is the contact field at Fe^{57} for a "free" Fe^{3+} ion with $S=\frac{5}{2}$. H^{dil}_{cov} is the contribution of covalent interactions to H_{hf} at Fe^{3+} in a nonmagnetic host, i.e., a magnetically dilute solid at infinite dilution. H^{dil}_{cov} arises principally from overlap and covalent interactions of the Fe^{3+} ions with its ligand neighbors. The net effect of this interaction is to transfer spin density from the 3d orbitals of the Fe^{3+} ion to its neighboring ligands. H_{orb} is the contribution to the hyperfine field from the orbital angular momentum which can be nonzero when the site symmetry is less than cubic. The

sum of H_c, H_{cov}^{dil}, and H_{orb} would therefore be the hyperfine field at a Fe^{3+} ion including nonmagnetic host effects and would be analogous to H_{hf} at Fe^{3+} in hosts such as MgO, CaO, and Al_2O_3. Since the changes in the internuclear separation and average site symmetry are small for $Ni_{1-x}Zn_xFe_2O_4$, $0 \leq x \leq 1.0$, the sum of the first three terms in Eq. (8) can be regarded as being constant. The small variations in the internuclear separation are not expected to change this sum since the much larger variations in Fe^{3+}-O^{2-} internuclear separations in Al_2O_3 (1.91 Å), MgO (2.10 Å), and CaO (2.40 Å) lead to a variation in H_{hf} of less than 0.5%.[45] Therefore, we are concerned primarily with variations in the last three terms of Eq. (8) as a function of x. H_{zsd} is the zero-point spin deviation corrected for the fact that our measurement temperature is not 0 °K. H_{zsd} is expected to vary with the value of x. However, H_{zsd} is expected to be quite small even at its maximal value in the $Ni_{1-x}Zn_xFe_2O_4$ system.[43] Furthermore, its contribution to $H_{hf}(A)$ should be relatively constant; and it should decrease in algebraic value with increasing x for $H_{hf}(B)$, i.e., the absolute magnitude of $H_{hf}(B)$ should increase. However, $|H_{hf}(B)|$ is observed to decrease with increasing x (Figs. 10 and 12) and the contribution of H_{zsd} to $H_{hf}(B)$ is not an important one. H_{dip} is the dipolar contribution arising from other magnetic ions in the lattice. H_{dip} is a function of both the cation distributions and magnetic moments of the cations and is expected to vary with x. Because of the cation disorder it is not possible to perform accurate dipolar-lattice sums; this is not a serious obstacle, however, since calculations have been made for $Co_{1-x}Zn_xFe_2O_4$ which show that the primary effect of a nonzero H_{dip} is to introduce line broadening.[33] Furthermore, the line broadening is small and reaches a maximal value of ~5 kOe for $H_{hf}(B)$ and ~2 kOe for $H_{hf}(A)$. Therefore, of the last three terms in Eq. (7) which are expected to be sensitive to x, the major contribution to variations in H_{hf} mostly arises from H_{cov}^{conc}. H_{cov}^{conc} is the covalent contribution to H_{hf} occasioned by the fact that the magnetic ions are close neighbors. This term includes only those covalent interactions that lead to spin transfer between different magnetic ions. While it may be difficult in theoretical calculations to separate the contributions from H_{cov}^{dil} and H_{cov}^{conc}, the experimental determination of H_{cov}^{conc} is quite straightforward. It is clear from Eq. (7) and recent theoretical investigations[43,44] that

$$H_{sthf} \equiv H_{cov}^{conc} , \tag{8}$$

where H_{sthf} is the supertransferred hyperfine field. H_{sthf} is the change in hyperfine fields associated with spin charge transfer and overlap effects between magnetic ions via direct metal-metal transfers and the indirect anion-assisted transfers such as metal-oxygen-metal, akin to the well-known super-exchange interactions, as well as the much weaker metal-oxygen-metal-oxygen-metal exchange paths. We neglect the $B \rightarrow B$ transfer processes not because we believe them to be unimportant but rather because of the insurmountable difficulties associated with 90° B-B angles and the lack of any reliable theoretical estimates of spin-transfer coefficients for d^5 ions with this configuration. As in previously reported studies,[42-44] the predominant variations in H_{sthf} are believed to result from overlap and covalent spin charge-transfer interactions between the next-nearest-neighbor cation d orbitals, the nearest-neighbor ligand σ orbitals, and the $4s$ orbitals of the ion being considered, e.g., $Fe^{3+}(B)$.

The decrease in $H_{hf}(B)$ with increasing Zn content is readily explained, qualitatively, as resulting from the decrease in $H_{sthf}(B)$ when the magnetic Fe^{3+} A-site ions are replaced by nonmagnetic Zn^{2+}. The Mössbauer spectra of the present study have not been analyzed using the details of the microstatistics of the cation distributions; nonetheless, an approximate value of $H_{sthf}(B)$ per $Fe^{3+}(A)$ can be obtained using the relationships

$$\langle H_{hf}(x) \rangle_B = H_{NiFe_2O_4} - \sum_{n=0}^{6} I(n, x) \Delta H_{sthf}(A \rightarrow B, n) , \tag{9}$$

where $\langle H_{hf}(x) \rangle_B$ is the average value of H_{hf} at the B-site Fe^{3+} ions when the Zn content is x. $\Delta H_{sthf}(A \rightarrow B, n)$ is the decrease in $H_{NiFe_2O_4}$ when n A-site Fe^{3+} ions are replaced by n Zn^{2+} ions. If each A-site neighbor contributes independently to $\Delta H_{sthf}(A \rightarrow B, n)$, then $\Delta H_{sthf}(A \rightarrow B, n) = n \Delta H_{sthf}(A \rightarrow B, 1)$. $I(n, x)$ is the relative frequency of occurrence of a B-site Fe^{3+} ion having n A-site Zn^{2+} neighbors when the Zn content is x and is given by

$$I(n, x) = \binom{6}{n} (x)^n (1 - x)^{6-n} . \tag{10}$$

$H_{NiFe_2O_4}$ is the maximal value for H_{hf} of Eq. (7) and also includes any contribution to H_{cov}^{conc} ($\equiv H_{sthf}$) of $B \rightarrow B$ supertransferred hyperfine interactions. If we assume that $\Delta H_{sthf}^{Fe}(B \rightarrow B, n) = \Delta H_{sthf}^{Ni}(B \rightarrow B, n)$ for $x \leq 0.5$, then the $B \rightarrow B$ contribution to $H_{sthf}(B)$ will be independent of x and constant. For $x > 0.5$, the above assumption is expected to be inappropriate. This is demonstrated by the onset of spin canting and the change in the functional dependence of H_{hf} on x. We can therefore determine $\Delta H_{sthf}(A \rightarrow B, 1)$ from two measured values of $\langle H_{hf}(x) \rangle_B$. For this purpose we chose x values of 0 and 0.3, and we obtain a value of 12 kOe for $\Delta H_{sthf}(A \rightarrow B, 1)$. Thus the total contribution to H_{cov}^{conc} ($\equiv H_{sthf}$) in pure $NiFe_2O_4$ is 72 kOe. This result confirms previous estimates of $\Delta H_{sthf}(A \rightarrow B, 1)$ based on extrapolation to 0 °K of values of $\langle H_{hf}(x) \rangle_B$ obtained at higher temperatures.[43]

We do not observe an increase in $H_{hf}(A)$ as the Fe^{3+} concentration on the B site is increased, as previously mentioned (cf. Fig. 10) and our observation of a rather constant $H_{hf}(A)$ up to $x \sim 0.8$ is unexpected in view of the strong dependence of $H_{hf}(B)$ on Zn content. The weak dependence of $H_{hf}(A)$ on the concentration of nonferric ions on the B site is not due wholly to the large number of B-site neighbors; the $\Delta H_{sthf}(1)$ contribution of $Fe^{3+}(B)$ to H_{hf} of $Fe^{3+}(A)$ is about three times less than that of $Fe^{3+}(A)$ to H_{hf} at $Fe^{3+}(B)$ even when the statistical considerations of the cation distributions are treated rigorously.[31a] So far, this behavior of $H_{hf}(A)$ is not understood; the results of the present study do indicate the general occurrence of this behavior and the need for a nonmaterial-specific explanation.

From overlap considerations, it is likely that the B-B spin-transfer processes are also important in determining the variations of $H_{hf}(B)$; but unfortunately, the Fe^{3+}-O-Fe^{3+} linkage angles are 90° and very little is known about the spin-transfer processes among d^5 ions for this geometry.

An indication that the contribution of B-B interactions to H_{sthf} is not entirely negligible is provided by the rate of change in $H_{hf}(B)$ as a function of x: Note that in Fig. 10 the decrease is linear for $x \leq 0.5$ but not for $x > 0.5$ and that this is also the x value at which the canting of the B-site Fe spins becomes observable. It is reasonable to suspect that this nonlinearity is due to a change in the B-B supertransferred hyperfine interactions as a consequence of the canting of B-site Fe moments.

V. SUMMARY

The cation distributions in $Ni_{1-x}Zn_xFe_2O_4$ for $0 \leq x \leq 1$ have been determined and shown to be the same as those expected on the basis of site-preference energies. Quantitatively, the cation distribution is $(Fe_{1-x}Zn_x)[Fe_{1+x}Ni_{1-x}]O_4$ for all values of x in the interval $0 \leq x \leq 1$.

At 7 °K, fluctuations, whether dynamic or static, in the magnitudes of the A- and B-site hyperfine fields are not very large and are qualitatively consistent with the predictions of a local-molecular-field model, taking into consideration long-range exchange coupling. The static fluctuations in the A-site hyperfine field are less than those in the B-site field, but the fluctuations at both sites reach a maximum at $x \approx 0.8$ at which value of x there may be fundamental change in magnetic structure. There is a decrease in the magnitude of the B-site hyperfine field, which is not expected on the basis of a local-molecular-field model, and which cannot be due to variations in T/T_N since $T/T_N < 0.01$ for most of the samples studied. We interpret this decrease as being due to changes in the supertransferred hyperfine fields. The relatively constant value of the hyperfine field at the A-site Fe^{3+} ions, however, requires further development in the overlap and covalence mechanism of supertransferred hyperfine interactions, at least for the spinel ferrite. There are no significant variations in [I.S. (A) − I.S. (B)] throughout the range of x values, and this is consistent with the quantitative crystal chemistry of these materials.

A Yafet-Kittel-type spin arrangement has been demonstrated for the Ni-Zn ferrites, as also indicated by other investigators. One of the more important results of this study, we feel, has been the discovery that the average canting angle of the B-site Fe spins is different from the average canting angle of all the B-site spins. The difference between the values for the canting angles is shown to be consistent with existing ideas concerning the relative strengths of the Fe-O-Fe and Ni-O-Fe exchange interactions. It has also been shown that there is no significant canting of the Fe^{3+} spins below an x value of 0.5. The canting angles derived from neutron-diffraction measurements for $x < 0.5$ must therefore be attributed to the Ni^{2+} spins if, in fact, there is any canting at all. The three-sublattice model of Satya Murthy *et al.*[11] has been shown to be only partly correct. The net B-site moment does not appear to be collinear with the A-site moment for $x \geq 0.7$. Indications are that both the A- and B-site moments are canted with respect to the net moment, but only the Fe^{3+} B canting angles have been determined in the present study due to poor resolution of the 2–5 lines and the weakness of the A site contribution to these lines. This canted spin structure is expected to be similar to that derived for $NiFe_{1.3}Cr_{0.7}O_4$[1] and $Co_{1-x}Zn_xFe_2O_4$.[33] The canting angles of the Fe^{3+} moments are less than those for the Ni^{2+} moments, as expected on the basis of the strengths of the Ni^{2+}-Fe^{3+} exchange interactions.

ACKNOWLEDGMENTS

The experimental measurements for this paper were supported by the Defence Research Board of Canada under Grant No. 9510-56 and by an equipment grant from the Research Board of the University of Manitoba. Acknowledgment is made to the donors of the Petroleum Research Fund, administered by the American Chemical Society, for PRF Grant No. 1947-G2 which made the participation of one of the authors (B.J.E.) in this study possible.

[1] J. Chappert and R. B. Frankel, Phys. Rev. Lett. **19**, 570 (1967).

[2] G. A. Sawatzky, F. van der Woude, and A. H. Morrish, Phys. Lett. A **25**, 147 (1967).

[3]B. J. Evans, in *Proceedings of the Fourth Symposium on Mössbauer Effect Methodology*, edited by I. J. Gruverman (Plenum, New York, 1968), and references therein.
[4]L. Cser, I. Dezsi, I. Gladkih, L. Keszthelyi, D. Kulgawczuk, N. A. Eissa, and E. Sterk, Phys. Status Solidi **27**, 131 (1968).
[5]E. Wieser, V. A. Povitskii, E. F. Makarov, and K. Kleinstück, Phys. Status Solidi **25**, 607 (1968).
[6]I. Nowick, J. Appl. Phys. **40**, 872 (1969).
[7]U. König, Y. Gros, and G. Chol., Phys. Status Solidi 33, 811 (1969).
[8]V. F. Belov, N. S. Ovanesyan, V. A. Trukhtanov, M. N. Shipko, E. V. Korneev, V. V. Korovushkin, and L. N. Korablin, Zh. Eksp. Teor. Fiz. **59**, 1484 (1970) [Sov. Phys.-JETP **32**, 810 (1971)].
[9]S. Geller, H. J. Williams, G. P. Espinosa, and R. C. Sherwood, Bell Syst. Tech. J. **43**, 565 (1964).
[10]V. C. Wilson and J. S. Kasper, Phys. Rev. **95**, 1408 (1954).
[11]N. S. Satya Murthy, M. G. Nater, S. I. Yousef, R. J. Begum, and C. M. Srivastava, Phys. Rev. **181**, 969 (1969).
[12]V. I. Goldanskii, V. F. Belov, M. N. Devisheva, and V. A. Trukhtanov, Zh. Eksp. Teor. Fiz. **49**, 1681 (1965) [Sov. Phys.-JETP **22**, 1149 (1966)].
[13]J. M. Daniels and A. Rosencwaig, Can. J. Phys. **48**, 381 (1970).
[14]M. A. Gilleo, J. Phys. Chem. Solids **13**, 33 (1960).
[15]I. Nowik, J. Appl. Phys. **40**, 872 (1969).
[16]J. S. Smart, in *Magnetism*, edited by G. Rado and H. Suhl (Academic, New York, 1963), Vol. III, p. 63.
[17]U. König, E. F. Bertaut, Y. Gros, and G. Chol, Solid State Commun. **8**, 759 (1970).
[18]J. M. D. Coey, G. A. Sawatzky, and A. H. Morrish, Phys. Rev. **184**, 334 (1969).
[19]Performed in duplicate by Schwarzkopf Microanalytical Laboratories, New York, N. Y.
[20]Philips Electronics, Eindhoven, The Netherlands.
[21]Princeton Research Corp., Princeton, N. J.
[22]Elron, Haifa, Israel.
[23]Nuclear Data Corp. Model No. 2200.
[24]C. Guillaud and M. Roux, C.R. Acad. Sci. (Paris) **229**, 1133 (1949).
[25]K. A. Piskarev, Bull. Acad. Sci. USSR Phys. Ser. 23, 282 (1959).
[26]J. G. Booth and J. Crangle, Proc. Phys. Soc. Lond. **79**, 1271 (1962).
[27]M. J. D. Powell, Comput. J. **5**, 147 (1962).
[28]G. A. Sawatzky, F. van der Woude, and A. H. Morrish, Phys. Rev. **187**, 747 (1969).
[29]B. J. Evans, Ph.D. thesis (University of Chicago, 1968) (unpublished).
[30]B. J. Evans and S. S. Hafner, J. Phys. Chem. Solids **29**, 1573 (1968).
[31](a) B. J. Evans and L. J. Swartzendruber, J. Appl. Phys. **42**, 1628 (1971); (b) F. K. Lotgering, J. Phys. Chem. Solids **27**, 139 (1966); (c) G. Blasse, Philips Res. Rep. **20**, 528 (1965).
[32]H. Abe, M. Matsuura, H. Yasuoka, A. Hirai, T. Hashi, and T. Fukuyama, J. Phys. Soc. Jap. **18**, 140 (1963).
[33]G. A. Petitt and D. W. Forester, Phys. Rev. B **4**, 3912 (1971).
[34]J. P. Morel, J. Phys. Chem. Solids **28**, 629 (1967).
[35]H. Yasuoka, A. Hirai, M. Matsuura, and T. Hashi, J. Phys. Soc. Jap. **17**, 1071 (1962).
[36]B. Boucher, R. Buhl, and M. Perrin, Phys. Status Solidi **40**, 171 (1970).
[37](a) S. I. Youssef, M. G. Natera, R. J. Begum, B. S. Srinivasan, and N. S. Satya Murthy, J. Phys. Chem. Solids **30**, 1941 (1969); (b) P. Raj and S. K. Kulshreshtha, Phys. Status Solidi A **4**, 501 (1971).
[38]M. Rosenberg, S. Mandache, H. Niculescu-Majewska, G. Filotti, and V. Gomolea, J. Appl. Phys. **41**, 1114 (1970).
[39]B. J. Evans, H.-P. Weber, and S. S. Hafner, J. Chem. Phys. **55**, 5282 (1971).
[40]Y. Yafet and C. Kittel, Phys. Rev. **87**, 290 (1952).
[41]K. Motida and S. Miyahara, J. Phys. Soc. Jap. **28**, 1188 (1970).
[42]B. J. Evans and L. J. Swartzendruber, Phys. Rev. B **6**, 223 (1972).
[43]F. van der Woude and G. A. Sawatzky, Phys. Rev. B **4**, 3159 (1971).
[44]E. Simanek, N. L. Huang, and R. Orbach, J. Appl. Phys. **38**, 1969 (1967).
[45]S. Geschwind, in *Hyperfine Interactions*, edited by A. J. Freeman and R. B. Frankel (Academic, New York, 1967), p. 225.

PHYSICAL REVIEW B VOLUME 8, NUMBER 1 1 JULY 1973

Fitting of Several Fe-Based Metallic Compounds Results in an Isomer-Shift–Electronic-Configuration Diagram

G. A. Fatseas
Laboratoire de Magnétisme, Centre National de la Recherche Scientifique 1, Place Aristide Briand, 92 Bellevue, France
(Received 28 September 1972)

An "isomer-shift–electronic-configuration" diagram is proposed for metallic compounds of iron, formed by theoretical charge density of Wakoh and Yamashita and Danon's δ scale. On the basis of this diagram, we show, in disagreement with previous interpretations of Mössbauer data based on the Walker *et al.* diagram, that the small dispersion of δ values, observed for several metallic compounds of iron, does not necessarily mean that the number of $3d$ electrons is nearly constant.

The isomer shift δ obtained by Mössbauer-effect measurements[1] was originally calibrated,[2] in terms of $3d$-$4s$ configuration, from δ values of some typical ionic iron compounds and theoretical free-ion $\Psi_s^2(0)$ data.[3] This calibration, in its original[2] or in several other modified forms,[4–9] has been successfully used to interpret isomer-shift results of pure ionic or less ionic iron compounds. However, all of these treatments give higher s-electron densities, $(3d^6 4s^2)$[5,7] or $(3d^7 4s^1)$,[2] for